

Nernst effect in the vortex-liquid regime of a type-II superconductor

Subroto Mukerjee and David A. Huse

Department of Physics, Princeton University, Princeton, NJ 08544

(Dated: May 22, 2019)

We measure the transverse thermoelectric coefficient α_{xy} in simulations of type-II superconductors in the vortex liquid regime, using the time-dependent Ginzburg-Landau (TDGL) equation with thermal noise. Our results are in reasonably good quantitative agreement with experimental data on cuprate samples, suggesting that this simple model of superconducting fluctuations contains much of the physics behind the large Nernst effect observed in these materials.

PACS numbers:

The Nernst effect in the cuprate superconductors has recently become a focus of attention both experimentally [1, 2, 3, 4, 5] and theoretically [6, 7, 8, 9]. The Nernst effect is the electric field induced when the sample has a temperature gradient, ∇T , perpendicular to the magnetic field, H ; this electric field is perpendicular to both ∇T and H . For some cuprate superconductors the Nernst effect due to superconducting fluctuations is detectable at temperatures far above the transition temperature, T_c [3, 4]. Ussishkin et al. [7] calculated the Nernst effect due to superconducting fluctuations, obtaining results in quantitatively good agreement (in absolute units) with experimental data. They used the linearized time-dependent Ginzburg-Landau (TDGL) equation, which is identical to the Aslamazov-Larkin [10] approximation for the microscopically linearized (Gaussian) TDGL is applicable far enough above the mean-field transition temperature T_c^{MF} , where the order parameter fluctuations are small enough to neglect the nonlinear terms in the full Ginzburg-Landau free energy.

Prominent in the phase diagrams of the cuprate superconductors is the vortex liquid regime, where short-range superconducting correlations are strong, but the thermal fluctuations of the vortices disrupt the superconducting coherence on longer scales. The experimentally observed Nernst effect remains large in this regime [2, 3, 4, 5], and can be understood as the phase-slip voltage due to vortices being transported down the temperature gradient as heat carriers. This vortex liquid regime is not readily accessible to analytic calculations. However, the TDGL equation driven by thermal fluctuations can be numerically simulated in the vortex liquid.

In this Letter, we present the method for and results of simulations of thermoelectric transport in type-II superconductors in the vortex liquid regime. We simulate the TDGL equation with thermal noise. We work in the strongly type-II limit, $\kappa \gg 1$, where the magnetic field in the sample is assumed to be uniform and not fluctuating. Mostly we work in two dimensions, but we also examine the crossover from two-dimensional to three-dimensional behavior. The simulations have been performed throughout the vortex liquid regime. We show that our results are in reasonably good qualitative and quantitative agreement with available experimental Nernst-effect data on overdoped $\text{La}_{2-x}\text{Sr}_x\text{CuO}_4$ (LSCO) [5]. We also

discuss in brief the results of our simulations to model experiments on $\text{Bi}_2\text{Sr}_2\text{CaCu}_2\text{O}_{8+x}$ (BSCCO) [2].

The transport coefficients are defined by the linear response relations

$$\begin{aligned} J_{\text{tr}}^e &= \hat{\sigma} \nabla T \\ J_{\text{tr}}^Q &= \hat{\kappa} \nabla T; \end{aligned} \quad (1)$$

where J_{tr}^e and J_{tr}^Q are respectively the charge and heat transport current densities. The Onsager relation for the matrices of thermoelectric transport coefficients is $\hat{\kappa} = T \hat{\sigma}$. When the magnetic field is along the z -direction and the Hall effect is negligible (an approximation we make), the thermoelectric coefficient that enters in the Nernst effect is α_{xy} .

One way to obtain transport coefficients from a simulation is via the Kubo relations, thus measuring current-current correlations in the equilibrium dynamics. Alternatively, one can apply an electric field and/or a temperature gradient and measure the resulting currents. We have used both methods, finding that our implementation of the latter method gives higher signal-to-noise ratio per unit computer time in the regime we have been studying. However, measuring the transport currents is not straightforward, since in the presence of a magnetic field there are also diamagnetic charge and heat currents that flow without dissipation, and it is the total currents that are measured by the local current operators. Thus we must subtract these diamagnetic currents to measure the transport currents. The procedure we use for this is based on the work of Cooper et al. [11], who call these diamagnetic currents "magnetization currents".

The energy (E) current density is related to the heat and charge currents by

$$J^Q(\mathbf{r}) = J^E(\mathbf{r}) - (\mathbf{r} \cdot \nabla) J^e(\mathbf{r}); \quad (2)$$

This relation holds for the total currents, J_{tot} , as well as for the transport currents alone, J_{tr} . We use a gauge where the vector potential is time-independent, so the electric field is $\mathbf{E} = -\nabla \phi$. For a sample with edges and in a uniform external magnetic field, it can be shown [11] that the diamagnetic parts of the charge and energy fluxes (but not the heat flux) vanish when one integrates the corresponding magnetization currents across

the whole sample, including its edges. Thus the transport part of the energy current is given by integrating the total energy current density across the sample:

$$I_{tr}^E = \int_S \int_{-Z}^Z J_{tr}^E(r) dS = \int_S J_{tot}^E(r) dS; \quad (3)$$

and similarly for the charge current. The integrals here are over a surface S cutting across the whole sample. Using this, we can then write the transport part of the heat current as

$$I_{tr}^Q = \int_S \int_{-Z}^Z J_{tot}^E(r) dS - \int_S (r) J_{tr}^e(r) dS; \quad (4)$$

We use a sample that has periodic boundary conditions along the x -direction (and along z when we study 3D) and free surfaces normal to \hat{y} . The magnetic field is along \hat{z} . To measure $\tilde{\kappa}_{xy}$ we apply an electric field along \hat{y} and measure the heat transport current along \hat{x} in the absence of any temperature gradient. If the system does not have a Hall effect, the x component of the electric transport current vanishes under these conditions, so does not contribute to the heat current. Then, using a surface S across the sample that is normal to \hat{x} , we have

$$\tilde{\kappa}_{xy} = \frac{I_{tr}^Q}{A r_y} = \frac{1}{A} \frac{\int_S J_{tot,x}^E(r) dS}{r_y}; \quad (5)$$

where A is the area (length in 2D) of the surface S across the sample. Similarly, $\tilde{\kappa}_{xy}$ is measured by introducing a temperature gradient along \hat{y} with no electric field, and measuring the charge transport along \hat{x} :

$$\kappa_{xy} = \frac{I_{tr}^e}{A r_y T} = \frac{1}{A} \frac{\int_S J_{tot,x}^e(r) dS}{r_y T}; \quad (6)$$

We can thus obtain the transport coefficients by measuring total currents in the system.

The TDGL equation that we have simulated is

$$\left(\partial_t + i \frac{e}{\hbar} \mu \right) \psi = \frac{\hbar^2}{2m} \nabla^2 \psi - \frac{e}{\hbar} A \psi + \frac{1}{a_0} \left(T - T_c^{MF} \right) \psi + \zeta(r;t); \quad (7)$$

We take μ to be real so there is no Hall effect [6]. The noise correlator is

$$\langle \zeta(r^0;t^0) \zeta(r;t) \rangle = 2 \frac{k_B T}{\hbar} \delta(r - r^0) \delta(t - t^0); \quad (8)$$

The current operators we need are

$$J_{tot}^e = \frac{e}{2m} \hbar \nabla \psi^\dagger \psi - \frac{ie}{\hbar} A \psi^\dagger \psi + c.c.; \quad (9)$$

$$J_{tot}^E = \frac{\hbar^2}{2m} \nabla \psi^\dagger \nabla \psi - \frac{ie}{\hbar} A \psi^\dagger \psi + c.c.;$$

It is important to note that the parameter ξ , which sets the time scales in this model, does not enter in the values

of the transverse thermoelectric coefficients we are studying, $\tilde{\kappa}_{xy}$ and $\tilde{\kappa}_{xy}$. This allows quantitative comparison to experiments to be done without estimating ξ , whose value is quite uncertain.

This TDGL equation with noise has a dimensionless parameter that gives the strength of the thermal fluctuations. To remove all the dimensional quantities, we use ξ_0 , the zero temperature coherence length, as our unit of length; T_c^{MF} , $k_B T_c^{MF}$, $\frac{\hbar^2}{2m}$ and $\frac{e}{\hbar} A$ ($a_0 T_c^{MF}$) as our units of temperature, energy, magnetic flux and time, respectively; and ξ_0 , the zero-temperature order parameter magnitude, as our unit for the order parameter. The resulting TDGL equation is then

$$\left(\partial_t + i \right) \psi = \left(\nabla^2 - A \right) \psi - \left(T - 1 \right) \psi + \zeta(r;t); \quad (10)$$

with noise correlator

$$\langle \zeta(r^0;t^0) \zeta(r;t) \rangle = 2 T \delta(r - r^0) \delta(t - t^0); \quad (11)$$

and

$$= \frac{k_B T_c^{MF}}{d (a_0 T_c^{MF})^2} \quad (12)$$

is the fluctuation parameter, where d is the number of spatial dimensions. When $d=1$, the actual critical temperature T_c is near the mean-field critical temperature T_c^{MF} , while if $d=3$ then $T_c < T_c^{MF}$. The model has four parameters that remain after scaling to the units specified above: the temperature, the magnetic field, the cutoff ξ , and the strength of the noise.

We initially simulate a two-dimensional system, thus ignoring interlayer coupling. We discretize space and time. The spatial grid spacing is taken to be ξ_0 . [This rather coarse spatial grid is used to allow us to simulate samples large compared to this microscopic length. There are noticeable effects of using such a coarse grid. For example, in our units $H_{c2}(T=0) = 1.18$ with this grid, while it is 1.0 for the continuum model. However, we expect that the effects of the discretization are only quantitative changes of this order and the qualitative behavior is not altered in the regime we study.] The time step is chosen to be between 0.02 and 0.1 in our units, with shorter steps at higher temperatures; we check that our results are not affected by doubling the time step. A first-order Euler method is used, with 10000 to 20000 time steps used for equilibration, and 30000 to 50000 steps for averaging. The two-dimensional data we show are for a 50 \times 50 square grid. We use the gauge-invariance of the TDGL equation to work as much as possible in terms of gauge-invariant quantities.

At $H = 0$ there is a Kosterlitz-Thouless [12] transition at T_c , which we locate by measuring the helicity modulus.

To obtain $\tilde{\kappa}_{xy}$, we measure the transverse energy current due an electric field. We then use the Onsager relation to obtain $\tilde{\kappa}_{xy} = \tilde{\kappa}_{xy} T$. We find that the signal to noise ratio for this measurement is significantly smaller than in a direct measurement of $\tilde{\kappa}_{xy}$. We have

numerically verified the validity of this Onsager relation by measuring α_{xy} both ways. This also serves as a check that we are indeed measuring the proper transport coefficients. We also confirm that our results agree with the analytic results [7] in the higher-temperature regime where linearized TDGL applies.

Some results for α_{xy} from the two-dimensional simulations are shown in Fig. 1. We have chosen to compare these results to the experimental results of Wang et al. [5] obtained from Nernst and resistivity measurements on an overdoped LSCO sample with $x = 0.2$ and $T_c = 28\text{K}$. For this comparison, we present the simulation results in SI units using the parameters from the experiment, $H_{c2}(T = 0) = 45\text{T}$ (thus $\Phi_0 = 27\text{A}$) and layer spacing $s = 6.6\text{\AA}$. The fluctuation parameter has been adjusted to $\beta = 0.42$ to give good quantitative agreement between simulation and experiment. We set the temperature scale using $T_c^{MF} = 40\text{K}$, which gives $T_c = 28\text{K}$ in the simulation. Note that α_{xy} is not directly measured in the experiments. For a system with negligible Hall effect, α_{xy} can be obtained from the measured Nernst effect and longitudinal resistivity. Thus for this comparison we require both these measurements to be made on the same sample over a substantial portion of the vortex liquid regime. This requirement seriously limits the number of experimental results we can compare to.

Looking at Fig. 1, we see that there is surprisingly good general qualitative and quantitative correspondence between the simulation and experiment, considering how simple the model is and that we have adjusted only the strength of the thermal fluctuations to get this agreement. The other parameters are all dictated by experiment. Our results are thus consistent with the proposition that the superconducting fluctuations modelled by the TDGL equation produce most, if not all, of the contributions to the large Nernst effect seen in the vortex liquid regime for this cuprate sample. Of course, the agreement between experiment and this simple model is not perfect. One difference is seen at high field in the higher-T panel of Fig. 1, where the simulations give a nearly-constant α_{xy} , while the experiment shows more variation.

One effect that is not included in our two-dimensional simulations is interlayer coupling. For the cuprates, this can become important in the vortex liquid at low fields in the vicinity of T_c , where there is a crossover to three-dimensional behavior as the correlation length normal to the layers becomes larger than one layer spacing. Note the maximum in the experimental α_{xy} in Fig. 1 for $T = 24\text{K}$ at about $H = 3\text{ Tesla}$. This peak and the decrease of α_{xy} for lower fields may be due to the crossover to three-dimensional behavior, and is not present in our two-dimensional simulation. To investigate this crossover, we have simulated the Lawrence-Doniach [13] version of the TDGL equation. In our units

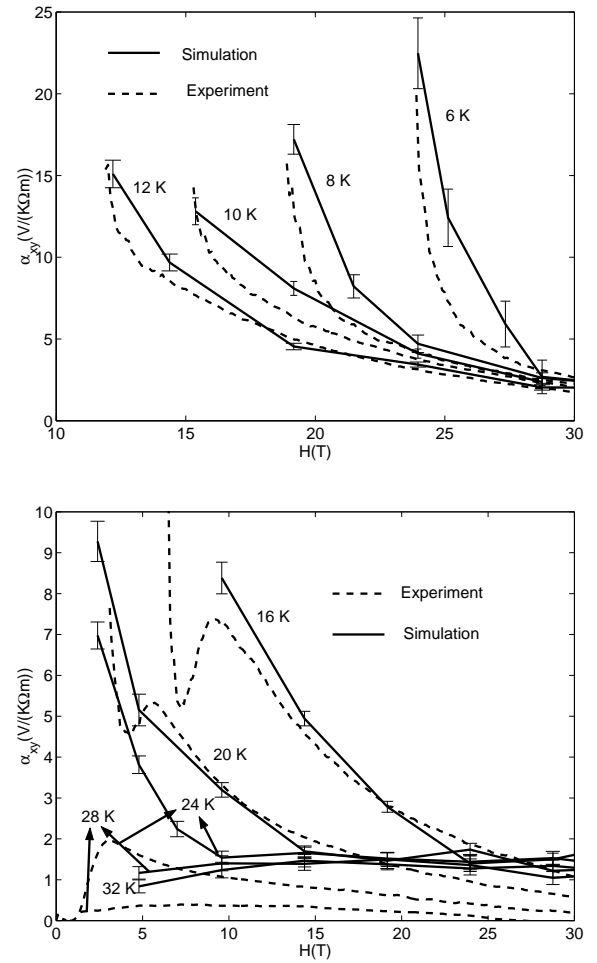


FIG. 1: Experimental data obtained from measurements [5] of the Nernst effect on overdoped LSCO ($x = 0.2$) along with the results of our two-dimensional simulations. The parameters used in the simulation are: $T_c^{MF} = 40\text{K}$, $H_{c2}(0) = 45\text{T}$, $s = 6.6\text{\AA}$, $\beta = 0.42$. The critical temperature is $T_c = 28\text{K}$ in both simulation and experiment here.

this is

$$\begin{aligned}
 (\partial_t + i) j = & (r_j - iA_j)^2 j - (T - 1) j \quad (13) \\
 & + J (e^{isA z_{j+1}} + e^{isA z_{j-1}} - 2 j) \\
 & + j j^2 j + ;
 \end{aligned}$$

where J is the interlayer Josephson coupling per unit area, and j is the layer index. The transition temperature is located by looking at the intersections of the fourth-order cumulant curves $\langle j^4 \rangle = \langle j^2 \rangle^2$ for different system sizes as functions of temperature at zero magnetic field. Fig. 2 shows results for α_{xy} as a function of field for various values of J at temperature $T = 24\text{K}$, from samples of size $15 \times 15 \times 10$ layers. For each J we set the temperature scale (T_c^{MF}) so that $T_c = 28\text{K}$ as in the experiment. The values of the other parameters in the simulations are as used in Fig. 1. As expected, the deviation from the two-dimensional behavior increases

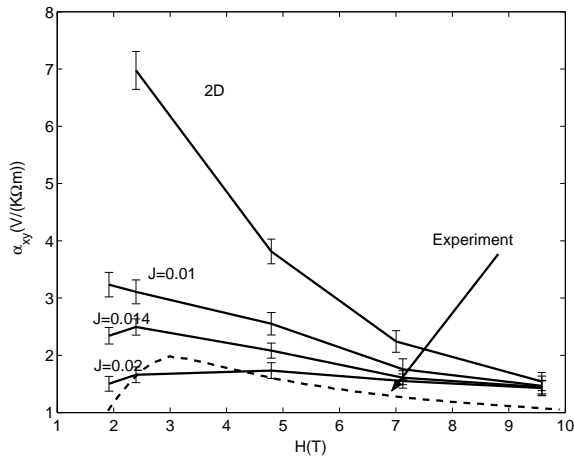


FIG. 2: Three-dimensional simulation results for $T = 24\text{K}$, with interlayer coupling J . See text for more details.

with the interlayer coupling J . A maximum in α_{xy} does appear, as in the experimental data, although this maximum appears to be sharper in the experiment than it is in the simulations.

An interesting point to note in Fig. 2 is that at low fields a rather small interlayer coupling J produces a strong decrease in α_{xy} . Describing this in terms of vortices, as seems appropriate in this low-field regime below T_c , the force per unit length on a vortex line due to the temperature gradient is proportional to α_{xy} . Naively, this force is also set by the entropy per unit length transported by a moving vortex. This transport entropy may come from internal degrees of freedom within one vortex, or it may come from the configurational entropy of the many possible spatial arrangements of the vortices. The latter does not involve internal excitations within the vortices. In the quasi-two-dimensional layered superconductors that we are modelling, a vortex line running normal to the layers consists of "pancake vortices" in each layer. A weak interlayer coupling has little effect on the internal properties of a single pancake vortex, but it does produce an attraction between vortices in adjacent layers

that reduces their relative motion, and thus can substantially reduce the configurational entropy of the vortices. The fact that at low fields a weak interlayer coupling greatly reduces the transport entropy of the vortices, as indicated by the reduction of α_{xy} seen in Fig 2, thus suggests that in this regime the configurational entropy of the vortices is a large part of their transport entropy, at least within this layered TDGL model.

We also performed simulations (results not shown here) to model the BSCCO sample studied by Riet al. [2]. They reported the transport energy of the vortices, defined as $U = T_0 \alpha_{xy}$. We used a 2d simulation with $T_c = 90\text{K}$, $H_{c2} = 160\text{T}$, $s = 15.35\text{Å}$ and $\kappa = 0.475$. Again, there was reasonably good quantitative agreement, in absolute units, between the experimental data and the simulations. The clearest deviation here occurred for $T < 60\text{K}$ and $H > 6\text{T}$, where the experimental α_{xy} has a much weaker T -dependence than in the simulations. This suggests that the TDGL model may be a poor approximation in some sense in this low- T , high- H part of the BSCCO phase diagram, perhaps due to quantum fluctuation effects.

In conclusion, we have demonstrated through numerical simulations that the TDGL equation with thermal fluctuations provides a reasonably good description of the transverse thermoelectric transport coefficient α_{xy} in the vortex-liquid regime of cuprate superconductors. We have seen that our simulations reproduce fairly well much of the qualitative and quantitative features of available experimental data. We have also studied the crossover from two-dimensional to three-dimensional behavior and found that features of the LSCO experimental data at low fields just below T_c might be attributed to this crossover. This crossover study also indicates that the configurational entropy of the vortices constitutes a large part of their transport entropy in this regime.

We thank Yayu Wang and N. P. Ong for providing us with the LSCO data. We also thank them, Shiva ji Sondhi and especially Iddo Ussishkin for many useful discussions. This work is supported by the NSF through MRSEC grant DMR-0213706.

-
- [1] T. T. M. Palstra, B. Batlogg, L. F. Schneemeyer and J. V. W. Aszczak, Phys. Rev. Lett. 64, 3090 (1990).
 [2] H. C. Ri, R. G. Ross, F. G. Polnik, A. Beck, R. P. Huebner, P. Wagner, and H. Adrian, Phys. Rev. B 50, 3312 (1994).
 [3] Z. A. Xu, N. P. Ong, Y. Wang, T. Kakeshita, and S. Uchida, Nature 406, 486 (2000).
 [4] Y. Wang, Z. A. Xu, T. Kakeshita, S. Uchida, S. Ono, Y. Ando, and N. P. Ong, Phys. Rev. B 64, 224519 (2001).
 [5] Y. Wang, N. P. Ong, Z. A. Xu, T. Kakeshita, S. Uchida, D. A. Bonn, R. Liang, and W. N. Hardy, Phys. Rev. Lett. 88, 257003 (2002).
 [6] S. Ullah and A. T. Dorsey, Phys. Rev. B 44, 262 (1991).
 [7] I. Ussishkin, S. L. Sondhi, and D. A. Huse, Phys. Rev. Lett 89, 287001 (2002).
 [8] I. Ussishkin, [cond-mat/0211384].
 [9] S. Tan and K. Levin, [cond-mat/0302248].
 [10] L. G. Aslamazov and A. I. Larkin (1968), [Sov. Phys. Solid State 10 875 (1968)].
 [11] N. R. Cooper, B. I. Halperin, and I. M. Ruzin, Phys. Rev. B 55, 2344 (1997).
 [12] J. M. Kosterlitz and D. J. Thouless, J. Phys. C 6, 1181 (1973).
 [13] W. E. Lawrence and S. Doniach, Proc. 12th Int. Conf. Low Temp. Phys., E. Kanda, ed. (Kyoto 1970, Keigaku Publ. Co. 1971), p. 361.